

Exploring the Leo II Dwarf Spheroidal: I. The Variable Star

Content

M. H. Siegel and S. R. Majewski¹

University of Virginia, Department of Astronomy

Received _____; accepted _____

arXiv:astro-ph/0004099v1 7 Apr 2000

¹David and Lucile Packard Foundation Fellow, Cottrell Scholar of the Research Corporation

ABSTRACT

We present the first comprehensive catalogue of variable stars in the Leo II dwarf spheroidal galaxy. We have identified 148 RR Lyrae type variables, of which 140 were amenable to derivation of variability parameters with our data. We have also confirmed the existence of four anomalous Cepheids as identified in previous studies.

The average period of the RR Lyrae ab variables (0.62 days), the fraction of c variables (0.24) and the minimum period of the RR Lyrae ab variables (0.51 days) all define Leo II as an “Oosterhoff intermediate” galaxy. We have used the properties of these variables to derive a metallicity for Leo II of approximately $[\text{Fe}/\text{H}]=-1.9$. We attempt to resolve discrepancies between this value and those determined by previous efforts. The presence of longer period, higher amplitude RR Lyrae variable implies a metallicity distribution that extends to as poor as $[\text{Fe}/\text{H}]=-2.3$.

Leo II’s location on the period-metallicity relation of clusters, like that of other “Oosterhoff intermediate” objects, falls between the Oosterhoff Class I and Oosterhoff Class II clusters. The properties of the variable populations of these objects are consistent with the idea that the Oosterhoff “dichotomy” is a continuum. The gap between the classes seems to be explained by the horizontal branch of Galactic globular clusters shifting away from the instability strip at intermediate metallicities. However, Leo II, as well as other Oosterhoff intermediate objects, has a second parameter effect strong enough to leave horizontal branch stars in the instability strip.

1. Introduction

The Leo II dwarf spheroidal galaxy (dSph) was first identified by Harrington and Wilson (1950) on the Palomar Sky Survey. Detailed information about Leo II did not appear in the literature for over three decades due to its extreme distance and small size (except the starcount study of Hodge 1962 and abstracts on variables in Swope 1967 and Swope 1968). A wave of interest in the 1980's (Hodge 1982; Demers and Harris 1983, hereafter DH83; Aaronson et.al. 1983; Azzopardi et al. 1985; Suntzeff et al. 1986, S86) revealed Leo II to be a metal-poor, second-parameter horizontal branch object with a handful of carbon stars.

Recently, a series of studies have expanded our knowledge of the Leo II system. Demers & Irwin (1993, DI93) with deep BV CCD photometry, derived a metallicity of $[\text{Fe}/\text{H}] = -1.9$ and revised Leo II's distance to 215 kpc. This was followed by the VI CCD studies of Lee (1995, hereafter L95) and Mighell & Rich (1996, hereafter MR96). The former derived a metallicity of -1.97 while the latter derived a metallicity of -1.6 and determined that Leo II formed almost all of its stars between 7 and 14 Gyr ago. Both confirmed a distance modulus close to the DI93 value. Vogt et al. (1995) measured radial velocities in Leo II and derived a mass-to-light ratio of 11.1.

One of the gaps in our knowledge of Leo II remains its variable star content. The seminal work in this field was to be the comprehensive survey of Baade and Swope. Their collection of over a hundred Palomar 200-inch plates was intended to produce a complete catalogue of Leo II variables. Unfortunately, while the catalogue exists, it has not been published, nor has a rigorous analysis been applied to the data. Swope did publish two brief abstracts, one reporting the identification of 152 variables and period measurement for 76 (Swope 1967) and another reporting four anomalous Cepheids (Swope 1968). A later update by van Agt (1973) reported 64 Bailey (1902) type ab RR Lyrae stars, six type c

and an average ab period of 0.59 days. Neither report was considered complete by the authors and neither included coordinates, finding charts or light curves. DI93 reported the identification of 80 variable candidates, but did not have enough images to fit light curves.

In this paper, we publish the first comprehensive list of positively identified variable stars in Leo II. We have found 148 RR Lyrae variables, for which we have successfully derived periods and amplitudes for 140. The distribution of periods is very similar to other dSph galaxies, with a moderate fraction of RRc variables. All of our observations are consistent with an “Oosterhoff intermediate” classification for Leo II and this classification is exhibited on a star-by-star basis. We have also identified four anomalous Cepheid variables. The presence and characteristics of these populations confirm that Leo II is metal-poor with a large intermediate age population. The longest period RRab variables hint at the existence of Leo II stars as metal-poor as $[\text{Fe}/\text{H}]=-2.3$.

2. Observations and Reduction

We observed the Leo II dSph with the 4-meter Mayall telescope at Kitt Peak on UT 8-9 April 1997 and 22-23 February 1998. Both observing runs used the T2KB 2048² thinned CCD chip and standard Harris prescription UBV filters. Our first observing run used the old Mayall prime focus doublet corrector while our second used the new four-element corrector (now in use with the MOSAIC camera). To avoid the ghost image produced by the four-element corrector, the camera was mounted ten minutes off of the optical axis of the telescope. This increased the distortion of the images, but not to a level that was uncorrectable. All data were reduced by the standard CCDPROC pipeline in IRAF.¹

¹IRAF is distributed by the National Optical Astronomy Observatories, which are operated by the Association of Universities for Research in Astronomy, Inc., under

All four nights suffered from very non-photometric observing conditions. We are, however, able to transform every frame to an identical instrumental system by inter-comparing individual photometric measures from frame to frame. This correction was applied iteratively until the average frame-to-frame residuals were reduced to 0.001 magnitudes. The combined instrumental magnitudes have been calibrated to the BV data set of DI93 within 0.01 magnitudes by the application of zero point and color corrections.

$$m_V = V_{inst} - 0.29 - 0.12(B - V) + 0.12(B - V)^2$$

$$m_B = B_{inst} - 0.20 - 0.04(B - V) + 0.10(B - V)^2$$

This transformation does leave some non-linearity in the comparison (Figure 1). This non-linearity is approximately 0.1 magnitudes over the four magnitudes of comparison. This may be due to filter differences or a non-linearity in the CCD used in one of the two studies. Independent calibration of the data set will be clearly be required in the future. Because of this non-linearity, all variable measures and light curve determinations were made purely from the instrumental system. However, all average magnitudes and intensity-weighted mean magnitudes in our catalogues have been converted to the DI93 system via the equations listed above.

We found that a total of 72 Leo II UBV images were usable for photometry. All of these images were processed through DAOPHOT (Stetson, 1987) and ALLFRAME (Stetson, 1994). The *combined* photometry is complete to a depth of $B = V = 24.5$ with instrumental errors at the horizontal branch of Leo II ($V=22.1$) of $(\sigma_V, \sigma_B) = (0.008, 0.016)$. However, the *individual* images have a wide variation in quality. Their average completeness limit is $B = V = 23.5$ with individual frame errors of $(\sigma_V, \sigma_B) = (0.08, 0.06)$ at the horizontal branch.

Accurate stellar positions were derived by using the IRAF task TFINDER with the Hubble Space Telescope Guide Star Catalogue. We were able to derive centroids for eight HST-GSC stars in our central field and used these stars to derive an approximate plate solution. Color and magnitude effects on the derived positions have not been accounted for. The coordinates listed in our variable catalogues (Tables I and III) are accurate to within approximately $0.''5$. A CCD template image and the X-Y positions of the variable stars were submitted for electronic availability through the Astronomical Journal.

3. Light Curve Fitting

Our UBV data include 56 V band observations of Leo II. All but one of these were deep enough for reasonable photometry of the horizontal branch. Our observations also include thirteen usable B band observations and three usable U band observations, which we have excluded from the period fitting due to the very poor phase coverage of the images. A file containing the Julian dates and V magnitudes of all observations of our variables stars is available electronically through the Astronomical Journal.

To identify variables in our data, we used a slightly modified version of the Welch-Stetson (1993) variability index, adopted from that calculated in the DAOMASTER code included with ALLFRAME. We confined our variability search to V images, as they were more numerous and of better quality. Figure 2 shows the index vs. magnitude plot and our selection criteria ($\text{Index} \geq 3.0$). A limit of 3.0 was selected as the lowest index where most stars had clear light curves and below which significant numbers of spurious detections began. We restricted our attempts to fit light curves to stars that had at least twenty observations and had been observed in both runs.

Periods were identified by both Phase Dispersion Minimization (Stellingwerf 1978)

and Stetson’s (1996) modified version of the Lafler-Kinman index (1965). The IRAF version of PDM proved very useful for identifying true variables and revealing the nature of those variables. It was especially adept at narrowing the range within which to search for periods, at finding periods for the short-period variables, and at producing light curves. The modified LK method proved more effective with longer period stars. Once a family of reasonable periods was identified, we ran each through a χ^2 fitting routine to refine amplitudes and to break the degeneracies of equally suitable periods. This routine used the templates of Layden (1998) for RRab stars and a sinusoidal curve for RRc.

In almost all cases, an obvious best fit was obtained. In some cases, degeneracies remained. These occurred in two intervals - large degeneracies of 0.2-0.5 days and small degeneracies of 0.01-0.02 days. Large degeneracies could be broken by using the well-established differences between RRc, RRab and Cepheid stars (rise time, amplitude and color). Small degeneracies were slightly more difficult to break. We settled for the period giving the lowest χ^2 fit. This period was then varied by several 10^{-5} days to further improve the fit.

The greatest deficiency of this technique is that a star that is not sampled at or near the peak brightness (within 0.1-0.2 in phase) will not be amenable to fitting. In fact, for low amplitude variables, it may not even have the contrast in brightness to be flagged as a variable. We have attempted to increase the number of detected variables by lowering the variability index threshold to 2.0. Approximately 10-20 stars in this range are potential RR Lyrae variables based on their PDM spectra. However, the magnitude contrast over the light curve is so slight that solutions prove very degenerate, if they are obtainable at all. For some of these stars, different periods have a χ^2 value below 1.0, making them statistically equivalent. Rather than include a small number of very poor or very degenerate variables, we left any variable with an index below 3.0 out of our sample.

Classification of variables was straight-forward. The three types of variable stars that commonly occur in dSph galaxies are RR Lyrae type ab, RR Lyrae type c and anomalous Cepheids. All three objects have well-established loci in period–amplitude–luminosity–effective temperature–rise time space.

4. The Variable Star Catalogue

Our variable star catalogue (Tables I and III) lists two identification numbers. The first is a running number for the variables alone, beginning with the 80 candidates from DI93. The second is a corresponding number from our master photometry catalogue of Leo II. These ID numbers are from ALLFRAME and roughly correlate with magnitude. Periods, amplitudes and pulsation modes are listed for stars for which these parameters could be derived. Magnitudes for most of the variable stars are intensity-weighted mean magnitudes. They were derived by integrating the template light curve in 0.02 phase increments (the same phase increments used in the Layden templates). For variables for which no variability parameters could be derived, the average observed magnitude is given.

We have compared our catalogue of variable stars to the list of potential variable stars in DI93. Of the 80 potential variable stars, we recover 40 as RR Lyrae type ab, 13 as type c and six as unknown RR Lyrae-like stars. One other star is an anomalous Cepheid. The remaining fifteen are not variables according to our analysis although seven of these fifteen have variability indices between 2.0 and 3.0, which places them just below our selected variable envelope; these may be true variables of very low amplitude or variables which were not in optimal phase during our observations. Table II lists the variable candidates in DI93 that did not meet our variability criterion, along with their corresponding identification number in our master photometry catalogue and our Welch-Stetson variability index.

5. The RR Lyrae Variables

Figure 3 shows the amplitude-period distribution of the positively identified RR Lyrae variables in Leo II. Parameters of the variables are given in Table I while light curves are shown in Figure 4.

We note the well-established period-amplitude relationship in the type ab variables. The c variables are of nearly constant amplitude although there is some hint of the parabola-like shape predicted by Bono et al. (1997).

For eight variables with RR Lyrae-like variations we were unable to obtain satisfactory fits to their photometric data. These stars could potentially be Blazhko (1907) variables or double-mode pulsators (Cox et al. 1980; Sandage et al. 1981, hereafter SKS; Cox et al. 1983; Nemec 1985a). Our data are not sufficient for a more rigorous analysis of their light curves. We have identified an additional three variables that have a well-defined light curve in one epoch of data and a poorly defined one in the other. The likely explanation is that these are exhibiting the Blazhko effect. They are listed in Table I with the best fit that could be obtained to one epoch of photometric data; these stars are noted with a classification of “abb”.

5.1. Leo II’s Stellar Populations

Sandage (1993a, S93a) demonstrated that the shortest RRab period could be used to discern the location of the blue fundamental edge of the instability strip, which is a function of metallicity. Using his relation of

$$\log(P_{ab}) = -0.122 [\text{Fe}/\text{H}] - 0.500$$

and the shortest RRab period of 0.50692 days ($\log(P) = -0.295$), we derive a metallicity of -1.68 on the Butler-Blanco scale (Butler 1975; Blanco 1992). This scale is 0.2 dex richer than the standard Zinn-West (1984) scale, so we correct our metallicity to -1.88.² This is closer to the low metallicity of DI93 and other ground-based studies than the higher MR96 metallicity of $[\text{Fe}/\text{H}]=-1.6$. A missing variable with a period of 0.469 days would move the metallicity scale back to the MR96 value. Such a low value does not occur in any of our fitted RRab periods, nor in the degeneracies of our unfitted variables.

S93a also defined several other relations for metallicity determination, which we list in order of declining sensitivity of our data. The mean period of RRab variables is well defined by our data (0.619 ± 0.006 days). S93a defines several relations between average RRab period and metallicity. We have chosen the relationships for cluster variables in which the average period has not been corrected for number density across the instability strip. This relation is use parameters closest to the actual measured quantities:

$$\log \langle P_{ab} \rangle = -0.092 [\text{Fe}/\text{H}] - 0.389$$

This produces a Zinn-West metallicity of -1.96 ± 0.04 dex. The mean period of RRc variables (0.363 ± 0.008 days), via the relation:

$$\log \langle P_c \rangle = -0.119 [\text{Fe}/\text{H}] - 0.670,$$

produces a Zinn-West value of -1.93 ± 0.08 dex. Finally, the longest RRab period defines the red edge of the instability strip and thus the lower bound of metallicity. Our longest ab

²The Zinn-West scale has been examined by Carretta & Gratton (1997) and Rutledge et al. (1997) and has been shown to have non-linearity in comparison to their metallicity measures. While metallicity measurements in this paper use the Zinn-West scale, the non-linearity should have only a minor effect upon our conclusions.

period is 0.8081 days. The relation:

$$\log(P_{ab}) = -0.09 [\text{Fe}/\text{H}] - 0.280$$

produces a -2.08 dex (-2.28 on the Zinn-West scale) lower bound for $[\text{Fe}/\text{H}]$.

The beauty of the Sandage relations is that they are completely independent of photometric zero point, reddening or calibration. Our results are consistent with previous metallicity estimates of Leo II, which have usually been around $[\text{Fe}/\text{H}]=-1.9$ (DH83, S86, DI93, L95).

The notable exception to these consistent metallicity determinations is MR96. Their analysis showed that photometric contamination of the red giant branch by red clump stars could have shifted DI93’s estimated metallicity. However, MR96 also noted a 0.10 magnitude difference between their V magnitudes and those of DI93, which they attributed to inaccurate airmass estimates on the part of DI93, possibly as a result of the eruption of Mt. Pinatubo. We are puzzled by this explanation, since DI93 observed standard stars on the same nights as Leo II. Unless the distribution of Pinatubo debris were extremely inhomogenous, it should affect the extinction terms equally for both standard and Leo II stars. The MR96 explanation would require a conspiracy of higher extinction only during Leo II observations. L95 detected a smaller V band difference of 0.02 magnitudes in the brightness range of interest (both L95 and our own comparison show some non-linearity at the bright end of the DI93 CCD data). A zero point correction to the V and I magnitudes of MR96 might result in a shift of their color, which would produce a metallicity-reddening shift based on the MR96’s use of Sarajedini’s (1994) calibration technique. A shift of 0.06 in color would move the giant branch onto an $[\text{Fe}/\text{H}]=-1.9$ metallicity relation. In the MR96 analysis, this is a 6σ deviation. However, Stetson (1998) has shown that WFPC2 data’s best attainable photometric precision is approximately 0.02 magnitudes due to charge-transfer

efficiency problems in the detectors. When taken in quadrature with MR96's (very small) photometric scatter and the uncertainties of the HST zero points (Holtzman et al. 1995), we estimate the uncertainties to be more likely near 0.03-0.04 magnitudes. This would reduce the shift of MR96 zero points to a $1.5 - 2\sigma$ effect. Given the comparisons between the V band magnitudes of MR96, L95, DI93 and our own study, we find a systematic magnitude shift of the WFPC2 data to be a plausible reconciliation of all the metallicity measures of Leo II.

However, the existence of a more metal-rich population could be plausible if it is too young to have a significant RR Lyrae population. MR96 showed that the youngest stars in Leo II are 7 Gyr old, with a typical star having an age of 9 Gyr. This is less than what is generally thought to be the minimum age possible for an RR Lyrae star, 10-12 Gyr (Olszewski et al. 1987, O87).

It is not clear how much weight such an argument should be given. First, O87 and MR96 use different methods of analysis. O87 used the *BV* isochrones of Vandenberg and Bell (1985) and Vandenberg (1985). MR96 averaged eight different age estimates, ranging from 7 to 11 Gyr (their Table 5). Of these, the most comparable age indicator to that used in O87 are the Revised Yale Isochrones (Green et al. 1987) which produced an age of 10 Gyr, just inside the O87 RR Lyrae minimum age envelope. Second, Leo II is only 1-3 Gyr younger than the supposed RR Lyrae minimum age, a difference comparable to the uncertainties (2 Gyr in both cases). Finally, the lower bound of RR Lyrae ages has only been determined by the comparison of Lindsay 1 to other LMC clusters and such an important result will not be conclusive until a wider variety of clusters lacking RR Lyrae's have been studied. Until the issues involved with globular cluster ages are fully resolved - and more cluster ages are determined - the possibility of a young, more metal-rich, variable-less population remains open.

We are intrigued by the presence of ab variables with periods longer than what should be the red edge of an $[\text{Fe}/\text{H}]=-1.9$ population. These imply a population that is more luminous than the bulk of Leo II variables. To separate out the more luminous stars in Leo II cleanly, we have applied a period-shift analysis to our data (Sandage 1981a; Sandage 1981b; Carney et al. 1992).

Period shift is measured by comparison to a reference variable population. The usual candidate population is that of M3, for which Sandage (1982a, 1982b) derived a measure of $\Delta \log P = -[0.129A_B + 0.088 + \log P]$, where A_B is the amplitude in the B passband. However, we applied this formulation to the recent measurements of M3 variable periods and amplitudes by Caretta et al. (1999) and Kažuný et al. (1998) and found a period shift of 0.015 by the Sandage formulation. We are unable to explain this discrepancy but have corrected the period shift zero point to produce a $\Delta \log P$ of 0.000 for the new M3 data. We have also derived a conversion ratio of $A_B/A_V=1.21$. The resulting revised period-shift relations are:

$$\Delta \log P = -[0.129A_B + 0.112 + \log P]$$

$$\Delta \log P = -[0.156A_V + 0.112 + \log P]$$

Our $\Delta \log P$ values for Leo II from these relations are plotted in Figure 5.

The pulsation equation of Van Aldada & Baker (1971) is:

$$\log P_o = -1.772 - 0.68 \log\left(\frac{M}{M_\odot}\right) + 0.84 \log\left(\frac{L}{L_\odot}\right) + 3.48 \log\left(\frac{6500}{T_{eff}}\right)$$

Assuming a uniform mass, one can measure changes in luminosity by measuring the period and effective temperature of each star. Effective temperature can not be directly measured, but SKS showed that amplitude, specifically in the blue passband, can be used to measure effective temperature. The most recent revision of this relation is by Catelan (1998):

$$\frac{5040}{T_{eq}} = 0.868 - 0.084A_B + 0.005[Fe/H]$$

Where T_{eq} is the equilibrium temperature. Equilibrium temperature is not the same as effective temperature, but is very similar (Carney et al. 1992). This relation has only a weak dependence upon metallicity. By comparing the periods of two stars with identical amplitudes, we compare stars at identical temperatures. This enables us to measure differences in luminosity.

The resultant theoretical ΔM_V scale is on the right ordinate of Figure 5. While there is a large amount of scatter intrinsic to the period-shift measure (and our conversion of the relations to the V passband only amplifies this scatter) it is clear that the stars in Leo II are dominated by a population 0.08 magnitudes more luminous than the stars of M3 with a higher luminosity tail in the longer period variables.

To confirm the increased luminosity for the longer period variables, we have directly compared the apparent magnitudes of our higher period shift population to the bulk population. We find that the nine most shifted stars ($\Delta \log P < -.08$) in Figure 5 (excluding the two that clearly deviate from the main magnitude locus in Figure 8) average $0.09 \pm .03$ magnitudes brighter than the bulk of the RR Lyrae stars. This is smaller than the 0.2 magnitude difference implied by the period-shift analysis (see Figure 5), which indicates a difference in mass for the more extreme Leo II variables.

If we abandon the assumption of fixed mass and use differences in magnitude to constrain luminosity differences, we can measure the relative mass of each star by rewriting the pulsation equation as:

$$-0.68 \log \frac{M_{avg}}{M} = -0.336(m - m_{avg}) + \Delta \log P - \langle \Delta \log P \rangle$$

where M_{avg} is the average RR Lyrae mass, M is the mass of an individual star, m_{avg} and m are the average and individual apparent magnitudes, and $\langle \Delta \log P \rangle$ is the average period

shift in Leo II. Using this formulation, we estimate the second population of stars to be 13% less massive than the average Leo II RRab star.

While longer period variables can occur in the absence of metallicity effects (Lee & Carney, 1999a; Pritzl et al. 1999), this signature is also seen in Sculptor (Kaluźny et al. 1995, hereafter K95), which has a well-established spread in metallicity (Norris & Bessell 1978; Smith & Dopita 1983; Da Costa 1984; Da Costa 1988; K95; Majewski et al. 1999, hereafter M99; Hurley-Keller et al. 1999). This may warrant a closer look at the Leo II color-magnitude diagram to see if a dual metallicity model may be more appropriate, as in the case of Sculptor. While dramatic conclusions should not be drawn from a handful of unusual stars, if the increased luminosity is the product of metallicity alone, this second Leo II population would have a metallicity of $[\text{Fe}/\text{H}]=-2.3$ using the RR Lyrae luminosity calibration of Sandage (1993b).

5.2. Oosterhoff Classification

It has long been known that Galactic clusters fall into two categories based upon the properties of their RR Lyrae variables (Oosterhoff 1939; see also a history of this phenomenon in S93a and Smith 1995). The ratio of c to ab variables of 0.24, the average RRab period of 0.62 days, and the minimum RRab period of 0.51 days are hallmarks of an Oosterhoff classification for Leo II that is intermediate between OoI and OoII. This classification is also seen in the Sculptor dSph (K95), Sextans (Mateo et al. 1995), several Magellanic clusters (Bono et al. 1994) and possibly the Draco (Nemec 1985b), Carina (Saha et al. 1986) and Ursa Minor (Nemec et al. 1988) dSph's.

S93a argued that the Oosterhoff dichotomy is the result of a continuous change of RR Lyrae properties with metallicity. The gap between Oosterhoff classes would result from

Galactic clusters with metallicities between OoI and OoII having extreme blue horizontal branches that depopulate the instability strip (Renzini 1983; Castellani 1983). Leo II and other Oosterhoff objects, however, have a second parameter effect that populates the red end of the horizontal branch and the instability strip. Figure 6 plots the average $\log P$ periods and spectroscopic metallicities of the clusters listed in S93a and the intermediate Oosterhoff clusters and dSph’s listed above. The Oosterhoff intermediate objects fill in the gap between the Oosterhoff classes and fall close to the relation of S93a. This would support the Renzini-Castellani-Sandage explanation of the Oosterhoff dichotomy.

The one caveat to this conclusion is that the dwarf spheroidal galaxies show evidence of multiple populations (see a summary in Grebel 1997, Grebel 1998 and Mateo 1998). This may be reflected in the variables of Leo II as well as those of Sculptor, which has a metallicity distribution from $[\text{Fe}/\text{H}]=-1.5$ to -2.3 (Kałuzny et al. 1995; M99). In principle, one could revive the Oosterhoff dichotomy by supposing that Oosterhoff intermediate objects merely reflect a superposition of OoI and OoII populations.

We find this to be a dubious interpretation. In the first place, the four intermediate LMC clusters all clearly have single populations. Second, in the case of Leo II and Sculptor, the consistency between non-variable measures of metallicity and the S93a formulation for the RR Lyrae stars indicates that the less metal-poor population is the origin of the bulk of the variables.

A third argument against this can be seen in Figure 5. The period shift is also a useful measure of the Oosterhoff effect in individual stars. Both cluster stars and field stars exhibit the Oosterhoff dichotomy by avoiding $\Delta \log P$ values between -0.01 and -0.05 (Suntzeff et al. 1991). If the Oosterhoff intermediate objects are a superposition of OoI and OoII, the mean $\Delta \log P$ value may be in the forbidden zone but individual stars should avoid it. Clearly, just as the Oosterhoff dichotomy is exhibited for Galactic cluster and field stars on

a star-by-star basis, so do the variables of Leo II violate that dichotomy on a star-by-star basis. Our reformulation of the $\Delta \log P$ measure places 56 of our 106 RR Lyrae ab variables into the forbidden region. Using the classical $\Delta \log P$ formulation places 39 of our stars in this region.³

This by no means implies that metallicity is the only parameter that affects the bulk and individual properties of cluster RR Lyrae stars. Metallicity has been suggested as the primary factor because of the likely increase in RR Lyrae luminosity with declining metallicity, which would produce the Oosterhoff effect (SKS). Any other effect that increases RR Lyrae luminosity, including HB evolution, would also affect the properties of the variable stars (Lee, Demarque & Zinn 1990, LDZ). Evolution is apparently the best explanation for the deviation of M2 from the primary locus in Figure 6 (Lee & Carney 1999b). However, Figure 6 shows that metallicity is the “first parameter” of average RRab period.

5.3. Distance Modulus

RR Lyrae variables are a useful tool for measuring distance modulus. However, the only studies that could be used to calibrate our data to true apparent magnitudes (DH83, DI93, L95, MR96) also use the horizontal branch as a distance indicator. Adapting these other studies to calibrate our RR Lyrae mean magnitudes for the same purpose would be circular and pointless. However, if used in combination with other calibration techniques, our RR Lyrae variable photometry might eventually serve to refine Leo II’s distance measure.

More importantly, the metallicity spread in the RR Lyrae variables of the dSph galaxies could assist with the refinement of the $M_V - [Fe/H]$ relation. Similar efforts with the

³An identical argument is used by Mateo et al. (1995) to show that the RRab stars of Sextans are Oosterhoff intermediate.

globular cluster ω Centauri (Dickens 1989) have been inconclusive, possibly because of the complicating effects of evolution (Gratton et al. 1986; Lee 1991). It has been argued that there is no universal $M_V - [Fe/H]$ relation that is independent of the effect of evolution as expressed in horizontal branch morphology (LDZ; Clement & Shelton 1999; Lee & Carney 1999a; Demarque et al. 1999). Untangling the evolution–metallicity–absolute magnitude question, especially in the absence of direct spectroscopic measures of RR Lyrae metallicity, is well beyond the scope of this paper.

6. Anomalous Cepheids

Swope (1968) identified four anomalous Cepheid variables in Leo II. We have also identified four variables with parameters similar to Swope’s that are cleanly separated from the RR Lyrae locus in period–amplitude–magnitude–color–rise time space. Light curves and derived parameters are given in Figure 7 and Table III respectively. We have listed what we believe to be the correct cross-identifications to the anomalous Cepheids of the Swope study. However, her V1 and V51 are not clearly distinguishable in the absence of a finding chart.

The apparent magnitudes and periods of all RR Lyrae and Cepheid variables are plotted in Figure 7 with the fundamental and first overtone Cepheid pulsation lines from Nemec et al. (1994). We find three fundamental and one first overtone pulsators among the anomalous Cepheids.

The origin of anomalous cepheids and their implications are still poorly understood (c.f. Nemec et al. 1988; Mateo et al. 1995). They can be indicative of a 5-10 Gyr old population, which MR96 showed exists in Leo II. They can also be mass-transfer binaries, for which a specific ratio of $\sim 1 - 10$ for blue-stragglers to anomalous Cepheids is predicted (Renzini,

Mengel & Sweigart 1977). Our photometry of Leo II, at present, does not allow a robust estimate of the blue straggler content due to the rapidly declining photometric accuracy as the data approach the main-sequence turnoff. However, if the suggested ratio were to hold up, the deep photometry of MR96 would be expected to show 0.5-5 blue stragglers (normalizing to the ratio of horizontal branch stars in our study and MR96). Even a cursory glance at their Figure 4 reveals a much higher number of blue stragglers. However, it is unclear as to how centrally concentrated these objects are (the MR96 pointing is close to the center of Leo II). Only deep wide-field photometry of the entire dSph will give an accurate statistical handle on this question.

7. Conclusions

7.1. Leo II and the Oosterhoff Continuum

The RR Lyrae variables in Leo II place its dominant metallicity at $[\text{Fe}/\text{H}]=-1.9$. A handful of large $\Delta \log P$ stars appears to imply a lower metallicity population. This is not conclusive, but warrants a more comprehensive look at the color-magnitude diagram of Leo II, which we will perform in a future contribution. At present, we can make no contribution regarding Leo II's distance modulus due to the non-photometric conditions during our observations.

Leo II is Oosterhoff intermediate class, like several other objects, including a number of dSph galaxies. Its violation of the Oosterhoff gap is exhibited in both the bulk and individual properties of its RR Lyrae stars. The Oosterhoff intermediate objects fill in the Oosterhoff gap, and therefore support the interpretation that metallicity is the dominant parameter in determining average RRab period.

7.2. The Fornax-Leo-Sculptor Stream Revisited

Lynden-Bell (1982) was the first to note that the dSph galaxies appear to lie in two great streams in the sky. One of these streams appears to include the Fornax, Leo I, Leo II and Sculptor dSph galaxies. Majewski (1992) noted that Phoenix, Sextans and several second parameter objects also lie along this plane. Palma et al. (2000) found that the outermost ($R_{GC} > 25$ kpc) second parameter globular clusters have the highest probability of being aligned with one of the two streams. While such alignments could be coincidental, they could also result from a common formation mechanism, in which case one might expect some similarities in the stellar populations of brethren objects.

Comparisons between the populations of Leo II and Sculptor are possible from the available data. Both show a strong low metallicity ($[\text{Fe}/\text{H}]=-1.7$ in Sculptor), second parameter, Oosterhoff intermediate population. Both also show evidence of a less populous, even more metal-poor population. In Sculptor, this population does not have a second parameter effect and is spatially dispersed (M99). The presence of a spatial gradient in the horizontal morphology of Leo II (Da Costa et al. 1996) may indicate a similar abundance-HB morphology pattern to that observed in Sculptor.

Fornax also has multiple populations. While it is dominated by a population at $[\text{Fe}/\text{H}]=-1.5$, it shows evidence of populations from -0.7 to -2.2 in both its field star and globular cluster population (c.f. Buonanno et al. 1985; Beauchamp et al. 1995). The most metal-poor population, like that in Sculptor, is much more extended than the metal-rich populations (Grebel & Stetson 1998). One could envision a scenario in which Fornax, Leo and Sculptor all originated in a common $[\text{Fe}/\text{H}]\sim-2.3$, first parameter HB progenitor, then, after dissociation, each object followed its own star formation history. Alternatively, perhaps there is something fundamental about the “threshold” metallicity $[\text{Fe}/\text{H}]=-2.3$ in small stellar systems. We note that the lowest metallicities in the Milky Way globular cluster

system are also around $[\text{Fe}/\text{H}]=-2.3$ (Harris 1996).

Any firm conclusions about correlations between Leo II, Sculptor and Fornax must await the measurement of their absolute proper motions. This will be the single most powerful discriminant for or against a common history. However, the similarities between the most metal-poor populations in each of Leo II, Sculptor and Fornax are intriguing.

The authors would like to thank Marcio Catelan for reading this article before submission and providing many useful comments. We would also like to thank the anonymous referee for useful remarks. MHS was provided thesis travel support by NOAO. MHS and SRM were supported by awards from the David and Lucile Packard Foundation and the Research Corporation, as well as National Science Foundation CAREER Award grant, AST-9702521.

REFERENCES

- Aaronson, M., Olszewski, E. W. & Hodge, P. W. 1983, *ApJ*, 267, 271
- Azzopardi, M., Lequeux, J. & Westerlund, B. E. 1985, *A&A*, 144, 388
- Bailey, S. I. 1902, *Annals of Harvard College Observatory*, 38, 1
- Beauchamp, D., Hardy, E., Suntzeff, N. B. & Zinn, R. 1995, *AJ*, 109, 1628
- Blanco, V. 1992, *AJ*, 104, 734
- Blazhko, S. 1907, *Astron. Nachr.*, 175, 325
- Bono, G., Caputo, F. & Stellingwerf, R.F. 1994, *ApJ*, 423, 294
- Bono, G., Caputo, F., Castellani, V. & Marconi, M. 1997, *A&AS*, 121, 327.
- Buonanno, R., Corsi, C. E., Fusi Pecci, F., Hardy, E. & Zinn, R. 1985, *A&A*, 152, 65
- Butler, D. 1975, *ApJ*, 200, 68
- Carney, B. W., Storm, J. & Jones, R. V. 1992, *ApJ*, 386, 663
- Carretta, E. & Gratton, R. G. 1997, *A&AS*, 121, 95
- Carretta, E., Cacciari, C., Ferraro, F. R., Fusi Pecci, F. & Tescicini, G. 1998, *MNRAS*, 298, 1005
- Castellani, V. 1983, *MSAIt*, 54, 141
- Catelan, M. 1998, *ApJ*, 495, L81
- Clement, C. M. & Shelton, I. 1999, *ApJ*, 515, L85
- Cox, A. N., King, D. S. & Hodson, S. W. 1980, *ApJ*, 236, 219
- Cox, A. N., Hodson, S. W. & Clancy, S. P. 1983, *ApJ*, 266, 94
- Da Costa, G. S. 1984, *ApJ*, 285, 483 (D84)

- Da Costa, G. S. 1988, in IAU Symp. 126, The Harlow Shapley Symposium on Globular Cluster Systems in Galaxies, eds. J. E. Grindlay & A. G. D. Philip (Dordrecht: Kluwer), 217
- Da Costa, G. S., Armandroff, T. E., Caldwell, N. & Seitzer, P. 1996, *AJ*, 112, 2576
- Demarque, P., Zinn, R., Lee, Y. W. & Yi, S. 1999, *ApJ*, *accepted*
- Demers, S. & Harris, W. E. 1983, *AJ*, 88, 329 [DH83]
- Demers, S. & Irwin, M. J. 1993, *MNRAS*, 261, 657 [DI93]
- Dickens, R. J. 1989, in *The Use of Pulsating Stars in Fundamental Problems in Astronomy*, ed. E. G. Schmidt, (Cambridge: Cambridge University Press), p. 141
- Gratton, R. G., Tornambe, A. & Ortolani, S. 1986, *A&A*, 169, 111
- Grebel, E. K. 1997, *RvMA*, 10, 29
- Grebel, E. K. 1998, in IAU Symposium 192: The Stellar Content of Local Group Galaxies, eds. P. Whitelock & R. Cannon, ASP Conf. Ser. Vol 192, (San Francisco: ASP), p. 1
- Grebel, E. K. & Stetson, P. B. 1998, in IAU Symposium 192: The Stellar Content of Local Group Galaxies, eds. P. Whitelock & R. Cannon, ASP Conf. Ser. Vol 192, (San Francisco: ASP), p. 11
- Green, E. M., Demarque, P. & King, C. R. 1987, *The Revised Yale Isochrones and Luminosity Functions* (Yale University Observatory, New Haven)
- Harrington, R. G. & Wilson, A. G. 1950, *PASP*, 62, 118
- Harris, W.E. 1996, *AJ*, 112, 1487
- Hodge, P. W. 1962, *AJ*, 67, 125
- Hodge, P. W. 1982, *AJ*, 87, 1668

- Holtzman, J. A., Burrows, C. J., Casertano, S., Hester, J. J., Trauger, J. T., Watson, A. M. & Worthey, G. 1995, *PASP*, 107, 1065
- Hurley-Keller, D. , Mateo, M. & Grebel, E. K. 1999, *ApJ*, 523, L25
- Kałużny, J., Kubiak, M., Szymanski, M., Udalski, A., Krzeminski, W. & Mateo, M. 1995, *A&AS*, 112, 407 [K95]
- Kałużny, J., Hilditch, R. W., Clement, C. & Rucinski, S. M. 1998, *MNRAS*, 296, 347
- Lafler, J. & Kinman, T. D. 1965, *ApJS*, 11, 216
- Layden, A. C. 1998, *AJ*, 115, 193
- Lee, J. W. & Carney, B. W. 1999a, *AJ*, 118, 1373
- Lee, J. W. & Carney, B. W. 1999b, *AJ*, 117, 2868
- Lee, Y. W., Demarque, P. & Zinn, R. 1990, *ApJ*, 350, 155 [LDZ]
- Lee, Y. W. 1991, *ApJ*, 373, L43
- Lee, M. G. 1995, *AJ*, 110, 1155 [L95]
- Lynden-Bell, D. 1982, *Observatory*, 102, 202
- Majewski, S. R., 1992, *ApJS*, 78, 87
- Majewski, S. R., Siegel, M. H., Patterson, R. J. & Rood, R. T. 1999, *ApJ*, 520, L33 [M99]
- Mateo, M. 1998, *ARA&A*, 36, 435
- Mateo, M., Fischer, P. & Krzeminski, W. 1995, *AJ*, 110, 2166
- Mighell, K. J. & Rich, M. R. 1996, *AJ*, 111, 777 [MR96]
- Nemec, J. M. 1985a, *AJ*, 90, 240
- Nemec, J. M. 1985b, *AJ*, 90, 204
- Nemec, J. M., Wehlau, A. & de Oliveira, C.M. 1988, *AJ*, 96, 528

- Nemec, J. M., Nemec, A. F. L. & Lutz, T. E. 1994, *AJ*, 108, 222
- Norris, J. & Bessell, M. S. 1978, *ApJ*, 225, L49
- Olszewski, E. W., Aaronson, M. & Schommer, R. A. 1987, *AJ*, 93, 565
- Oosterhoff, P. Th. 1939, *Observatory*, 62, 104
- Palma, C., Majewski, S. R. & Johnston, K. V. 1999, *ApJ*, *submitted*
- Pritzl, B., Smith, H.A., Catelan, M. & Sweigart, A. V. 1999, *ApJ*, *accepted*
- Renzini, A., Mengel, J. G. & Sweigart, A. V. 1977, *A&A*, 56, 369
- Renzini, A. 1983, *MSAIt*, 54, 335
- Rutledge, G. A., Hesser, J. E. & Stetson, P. B. 1997, */pasp*, 109, 907
- Saha, A., Monet, D. G. & Seitzer, P. 1986, *AJ*, 92, 302
- Sandage, A., Katem, B. & Sandage, M. 1981, *ApJS*, 46, 41 [SKS]
- Sandage, A. 1981a, *ApJ*, 244, L23
- Sandage, A. 1981b, *ApJ*, 248, 161
- Sandage, A. 1982a, *ApJ*, 252, 553
- Sandage, A. 1982b, *ApJ*, 252, 574
- Sandage, A. 1993a, *AJ*, 106, 687 [S93a]
- Sandage, A. 1993b, *AJ*, 106, 703
- Sarajedini, A. 1994, *AJ*, 107, 618
- Smith, H. S. & Dopita, M. A. 1983, *ApJ*, 271, 113
- Smith, H. A. 1995, *RR Lyrae Stars* (Cambridge: Cambridge University Press)
- Stellingwerf, R. F. 1978, *ApJ*, 224, 953
- Stetson, P. B. 1987, *PASP*, 99, 191

- Stetson, P. B. 1994, *PASP*, 106, 250
- Stetson, P. B. 1996, *PASP*, 108, 851
- Stetson, P. B. 1998, *PASP*, 110, 1448
- Suntzeff, N. B., Aaronson, M., Olszewski, E. W. & Cook, K.H. 1986, *AJ*, 91, 1091 [S86]
- Suntzeff, N. B., Kinman, T. D. & Kraft, R. P. 1991, *ApJ*, 367, 528
- Swope, H. H. 1967, *PASP*, 79, 439
- Swope, H. H. 1968, *AJ*, 73, S204
- van Agt, S. 1973, in *Variable Stars in Globular Clusters and Related Systems*, ed. J. D. Fernie, (Dordrecht: Reidel), p. 35
- van Albada, T.S. & Baker, N. 1971, *ApJ*, 169, 311
- VandenBerg, D. A. & Bell, R. 1985, *ApJS*, 58, 561
- VandenBerg, D. A. 1985, *ApJS*, 58, 711
- Vogt, S. S., Mateo, M., Olszewski, E. W. & Keane, M. J. 1995, *AJ*, 109, 151
- Welch, D. L. & Stetson, P. B. 1993, *AJ*, 105, 1813
- Zinn, R. & West, M. J. 1984, *ApJS*, 55, 45

Fig. 1.— Comparison of stars from DI93 to the corrected B and V magnitudes of this study. While the comparisons have RMS values of 0.01 magnitudes, both show a degree of non-linearity in comparison.

Fig. 2.— V magnitude plotted against the modified Welch-Stetson index. All objects above the dashed line were marked as potential variables. While the bright end locus moves above this line, almost all of these objects had increase indices due to saturation effects.

Fig. 3.— Period-amplitude distribution of the variables in Leo II. *Boxes* are RRab variables, *circles* are RRc, *filled triangles* are anomalous Cepheids. Periods are in days.

Fig. 4.— RR Lyrae light curves in order of increasing period.

Fig. 5.— The period shift effect in the variables of Leo II. $\Delta \log P$ is the period shift. The right ordinate shows the corresponding magnitude shift, under the assumption of constant mass. The dashed lines mark the zone avoided by Galactic and cluster stars.

Fig. 6.— Average RRab period against spectroscopic metallicity for globular clusters and dwarf spheroidal galaxies with 10 or more measured RRab variables. *Circles* are OoI clusters, *open triangles* Oo intermediate and *squares* OoII. For this plot, we have adopted Draco as Oo intermediate, Carina and Ursa Minor as OoII. The solid line is the observational fit from Sandage (1993a). The significantly deviant point is M2, based on the study of Lee & Carney (1999b).

Fig. 7.— Light curves of the anomalous Cepheid variables in Leo II.

Fig. 8.— Apparent magnitudes of all variables stars within Leo II as a function of period. RRab variables are marked with *squares*, RRc with *circles* and anomalous Cepheids with *filled triangles*. The solid lines are the fundamental and first overtone modes produced by Nemec et al. (1994).

TABLE I. RR Lyrae Variables

Var ID	Star ID	RA J2000.0	DEC J2000.0	Period (Days)	A_V	m_V	Bailey Type	$\Delta \log P$
V1	2350	11:13:23.36	22:12:56.5	0.67352	0.723	22.08	ab	-0.053
V2	2755	11:13:32.25	22:12:13.1	0.62137	0.622	22.17	ab	-0.002
V5	4035	11:13:39.17	22:11:21.7	0.57152	0.967	22.20	ab	-0.020
V6	2597	11:13:42.30	22:10:58.6	0.64544	0.604	22.09	ab	-0.016
V8	2768	11:13:32.68	22:11:29.5	0.63715	0.757	22.17	ab	-0.034
V9	2153	11:13:27.92	22:11:43.3	0.62357	0.751	21.89	ab	-0.024
V10	3149	11:13:20.75	22:12:02.0	0.32033	0.769	22.13	c	
V11	3373	11:13:29.65	22:11:23.4	0.65546	0.619	22.24	ab	-0.025
V14	3735	11:13:25.80	22:11:38.0	0.64419	0.535	22.21	ab	-0.004
V15	2059	11:13:31.82	22:11:10.6	0.62126	0.997	22.16	ab	-0.061
V16	1892	11:13:35.79	22:10:53.0	0.39198	0.386	21.71	c	
V17	3262	11:13:41.16	22:10:18.9	0.56056	1.040	22.36	ab	-0.023
V18	2379	11:13:19.63	22:11:46.2	0.79279	0.571	22.09	ab	-0.100
V19	3316	11:13:34.28	22:10:37.0	0.40336	0.694	22.13	c	
V21	3217	11:13:38.10	22:10:11.8	0.65821	0.633	22.18	ab	-0.029
V22	1965	11:13:16.90	22:11:36.6	0.59125	1.017	22.08	ab	-0.042
V23	3144	11:13:41.58	22:09:40.3	0.53865	1.344	22.31	ab	-0.053
V24	4297	11:13:24.46	22:10:53.0	0.39538	0.636	22.28	c	
V25	3068	11:13:20.36	22:11:10.3	0.38665	0.547	22.27	c	
V28	3193	11:13:32.64	22:09:33.2			22.10	unk	
V29	2451	11:13:32.27	22:09:27.8	0.76034	0.747	22.18	ab	-0.110
V30	3230	11:13:30.71	22:09:17.3	0.57145	0.776	22.28	ab	0.010
V31	2676	11:13:35.88	22:08:47.6	0.36563	0.778	22.18	c	
V32	3992	11:13:19.63	22:09:55.9	0.38714	0.502	22.27	c	
V33	3273	11:13:28.22	22:09:17.8	0.63122	0.743	22.26	ab	-0.028
V34	2472	11:13:18.82	22:09:57.0	0.62329	0.643	22.05	ab	-0.007

TABLE I. Continued. RR Lyrae Variables

Var ID	Star ID	RA J2000.0	DEC J2000.0	Period (Days)	A_V	m_V	Bailey Type	$\Delta \log P$
V36	2770	11:13:26.43	22:09:14.0	0.61411	0.683	22.21	ab	-0.007
V37	4140	11:13:26.46	22:09:11.3	0.35721	0.497	22.28	c	
V38	3306	11:13:27.06	22:09:05.0	0.26012	0.489	22.16	c	
V39	3597	11:13:33.00	22:08:35.9	0.61989	0.450	22.20	ab	0.025
V40	2863	11:13:18.29	22:09:38.4	0.70926	0.510	22.01	ab	-0.042
V41	2598	11:13:29.06	22:08:48.6	0.59113	0.993	22.04	ab	-0.039
V43	3018	11:13:32.61	22:08:17.2	0.56856	0.758	22.23	ab	0.015
V44	3092	11:13:34.95	22:07:59.2	0.36896	0.559	22.16	c	
V46	4203	11:13:30.18	22:08:17.0	0.60083	0.942	22.21	ab	-0.038
V48	3159	11:13:24.68	22:08:37.9	0.70922	0.599	22.24	ab	-0.056
V49	2322	11:13:19.43	22:08:59.4	0.76280	0.583	22.02	ab	-0.085
V50	2736	11:13:16.78	22:09:08.6			22.00	unk	
V52	2409	11:13:23.49	22:08:35.1	0.55269	1.015	22.24	ab	-0.013
V54	4201	11:13:32.64	22:07:48.3	0.59702	0.711	22.26	ab	0.001
V55	2695	11:13:27.61	22:08:06.6	0.62718	1.020	22.30	ab	-0.069
V56	4058	11:13:28.52	22:08:01.5	0.34118	0.599	22.28	c	
V57	2696	11:13:17.33	22:08:43.8	0.42179	0.348	21.97	c	
V60	4354	11:13:27.22	22:07:51.8	0.60862	1.027	22.34	ab	-0.057
V61	2712	11:13:29.18	22:07:34.6	0.56883	0.810	22.20	ab	0.007
V62	2690	11:13:12.35	22:08:44.4	0.36202	0.601	22.17	c	
V64	4225	11:13:21.44	22:07:54.2			22.29	unk	
V65	3354	11:13:30.42	22:07:12.6	0.60716	0.686	22.21	ab	-0.002
V67	2459	11:13:17.38	22:07:54.3	0.56032	1.031	22.16	ab	-0.021
V69	3207	11:13:35.74	22:06:23.9			22.12	unk	
V70	3835	11:13:27.33	22:06:56.8	0.62026	0.725	22.22	ab	-0.018
V73	3236	11:13:13.22	22:07:48.7			22.11	unk	

TABLE I. Continued. RR Lyrae Variables

Var ID	Star ID	RA J2000.0	DEC J2000.0	Period (Days)	A_V	m_V	Bailey Type	$\Delta \log P$
V74	4029	11:13:27.42	22:06:39.2	0.59392	0.854	22.26	ab	-0.019
V75	3277	11:13:31.50	22:06:16.6	0.57313	1.003	22.17	ab	-0.027
V76	2669	11:13:10.62	22:07:47.1			22.06	unk	
V77	3611	11:13:10.70	22:07:43.8	0.65676	0.569	22.18	ab	-0.018
V78	4088	11:13:20.34	22:07:00.0	0.56884	0.706	22.25	ab	0.023
V79	3548	11:13:29.42	22:06:08.9	0.63790	0.787	22.07	ab	-0.040
V80	3875	11:13:34.82	22:05:33.7	0.57016	0.944	22.10	ab	-0.015
V81	1517	11:13:07.99	22:08:40.7	0.80097	0.735	21.56	ab	-0.130
V82	1675	11:13:27.46	22:07:27.7	0.39731	0.289	21.42	c	
V83	1770	11:13:36.13	22:15:51.1			21.57	unk	
V84	1784	11:13:43.00	22:07:26.4	0.60829	1.013	22.10	ab	-0.054
V85	1900	11:13:11.76	22:09:13.9	0.60888	1.080	22.08	ab	-0.065
V86	1922	11:13:43.72	22:10:48.4	0.28667	0.621	21.57	c	
V87	1982	11:13:33.26	22:10:23.6	0.53243	1.235	22.28	abb	-0.031
V88	1996	11:13:52.92	22:08:53.0	0.80806	0.546	21.74	ab	-0.105
V89	2025	11:13:48.63	22:10:13.3	0.56978	1.180	22.26	ab	-0.052
V90	2188	11:13:23.76	22:15:28.2	0.55128	1.208	22.26	ab	-0.042
V91	2230	11:13:15.20	22:04:26.6	0.36791	0.532	21.93	c	
V92	2269	11:13:16.10	22:03:55.2	0.39916	0.467	21.99	c	
V93	2290	11:13:44.23	22:05:27.8	0.28849	0.664	22.13	c	
V94	2300	11:13:13.55	22:05:53.4	0.60191	0.873	22.16	ab	-0.028
V95	2312	11:13:39.20	22:07:15.4	0.64360	0.757	22.07	ab	-0.039
V96	2334	11:13:19.34	22:07:55.6	0.40767	0.517	21.98	c	
V97	2382	11:13:40.25	22:07:43.3	0.37708	0.517	22.14	c	
V98	2394	11:13:39.79	22:07:45.7	0.58175	0.591	22.04	ab	0.031
V99	2448	11:13:37.13	22:13:44.0	0.54193	0.829	22.22	ab	0.025

TABLE I. Continued. RR Lyrae Variables

Var ID	Star ID	RA J2000.0	DEC J2000.0	Period (Days)	A_V	m_V	Bailey Type	$\Delta \log P$
V100	2467	11:13:18.04	22:07:58.8	0.51503	1.323	22.35	ab	-0.030
V101	2497	11:13:49.69	22:08:35.3	0.60588	0.779	22.13	ab	-0.016
V102	2561	11:13:15.43	22:10:09.7	0.52567	1.088	22.26	ab	-0.002
V103	2593	11:13:21.09	22:11:14.8	0.59649	0.997	22.25	ab	-0.043
V104	2607	11:13:40.42	22:08:34.6	0.77449	0.542	22.06	ab	-0.086
V105	2621	11:13:33.61	22:04:11.7	0.53191	1.066	22.19	ab	-0.004
V106	2633	11:13:21.18	22:10:59.2	0.67730	0.403	22.05	ab	-0.006
V107	2688	11:13:07.32	22:07:02.3	0.63038	1.166	22.03	ab	-0.093
V108	2716	11:13:48.58	22:15:11.1	0.62602	0.759	22.21	ab	0.027
V109	2767	11:13:22.05	22:11:29.5	0.58815	0.872	22.19	ab	-0.018
V110	2801	11:13:44.87	22:03:39.7	0.64623	1.130	22.25	ab	-0.099
V111	2820	11:13:28.25	22:07:08.2	0.28828	0.576	22.02	c	
V112	2830	11:13:14.64	22:09:38.2	0.34577	0.754	22.32	c	
V113	2871	11:13:33.23	22:12:45.3	0.67845	0.564	22.17	ab	-0.032
V114	2887	11:13:49.59	22:04:44.7	0.64921	0.709	22.03	ab	-0.035
V115	2896	11:13:29.42	22:08:23.6	0.66809	0.530	22.11	ab	-0.020
V116	2899	11:13:30.10	22:01:49.9	0.61526	1.214	22.08	ab	-0.090
V117	2906	11:13:35.27	22:07:34.5	0.64489	0.538	22.05	ab	-0.005
V118	2943	11:13:40.84	22:04:01.1	0.35405	0.559	22.18	c	
V119	2962	11:13:24.90	22:11:02.5	0.77051	0.361	22.13	ab	-0.055
V120	2990	11:13:15.84	22:12:59.7	0.65160	0.572	22.16	ab	-0.015
V121	3006	11:13:36.99	22:08:59.5	0.62537	0.689	22.03	ab	-0.016
V122	3031	11:13:28.43	22:04:49.6	0.53380	1.008	22.21	ab	0.003
V123	3055	11:13:46.00	22:07:26.9	0.63797	0.631	22.18	abb	-0.015
V124	3072	11:13:42.68	22:06:25.4	0.41264	0.460	22.09	c	
V125	3086	11:13:39.67	22:11:59.1	0.65294	0.771	22.09	ab	-0.047

TABLE I. Continued. RR Lyrae Variables

Var ID	Star ID	RA J2000.0	DEC J2000.0	Period (Days)	A_V	m_V	Bailey Type	$\Delta \log P$
V126	3121	11:13:20.53	22:07:13.3	0.58798	0.882	22.17	ab	-0.019
V127	3122	11:13:03.71	22:05:51.8	0.37047	0.580	22.15	c	
V128	3166	11:13:30.67	22:09:12.5	0.62768	0.857	22.10	ab	-0.043
V129	3180	11:13:30.03	22:05:22.6	0.54800	1.279	22.16	ab	-0.050
V130	3218	11:13:19.76	22:06:16.2			22.12	unk	
V131	3231	11:13:06.56	22:02:41.1	0.63519	0.889	22.11	ab	-0.054
V132	3240	11:13:36.35	22:09:04.3	0.32976	0.444	22.26	c	
V133	3257	11:13:40.16	22:06:16.4	0.66382	0.638	22.09	ab	-0.034
V134	3351	11:13:11.72	22:08:54.0	0.41174	0.592	22.10	c	
V135	3355	11:13:48.37	22:06:15.5	0.59801	0.967	22.21	ab	-0.040
V136	3363	11:13:34.75	22:07:44.2	0.58072	0.695	22.21	ab	0.016
V137	3419	11:13:32.00	22:10:50.2	0.54721	0.725	22.23	ab	0.037
V138	3470	11:13:46.51	22:12:51.0	0.57274	0.789	22.18	ab	0.007
V139	3603	11:13:39.59	22:12:06.3	0.37020	0.810	22.25	c	
V140	3612	11:13:38.01	22:06:10.5	0.57298	0.670	22.2	abb	0.025
V141	3648	11:13:12.49	22:04:50.4	0.53736	1.076	22.22	ab	-0.010
V142	3655	11:13:40.13	22:10:37.0	0.57900	0.806	22.17	ab	-0.000
V143	3668	11:13:42.93	22:07:37.7	0.67390	0.687	22.16	ab	-0.048
V144	3728	11:13:43.62	22:06:53.2	0.60467	0.824	22.15	ab	-0.022
V145	3753	11:13:23.40	22:06:11.7	0.30380	0.442	22.14	c	
V146	3756	11:13:10.54	22:04:10.3	0.62178	0.529	22.14	ab	0.012
V147	3767	11:13:20.15	22:05:44.6	0.39119	0.462	22.17	c	
V148	3793	11:13:22.04	22:10:54.7	0.59595	0.884	22.33	ab	-0.025
V149	3819	11:13:17.59	22:03:32.8	0.59440	0.980	22.20	ab	-0.039
V150	3827	11:13:44.15	22:14:33.2	0.63607	0.599	22.20	ab	-0.009
V151	3833	11:13:46.82	22:09:44.5	0.64002	0.674	22.17	ab	-0.023

TABLE I. Continued. RR Lyrae Variables

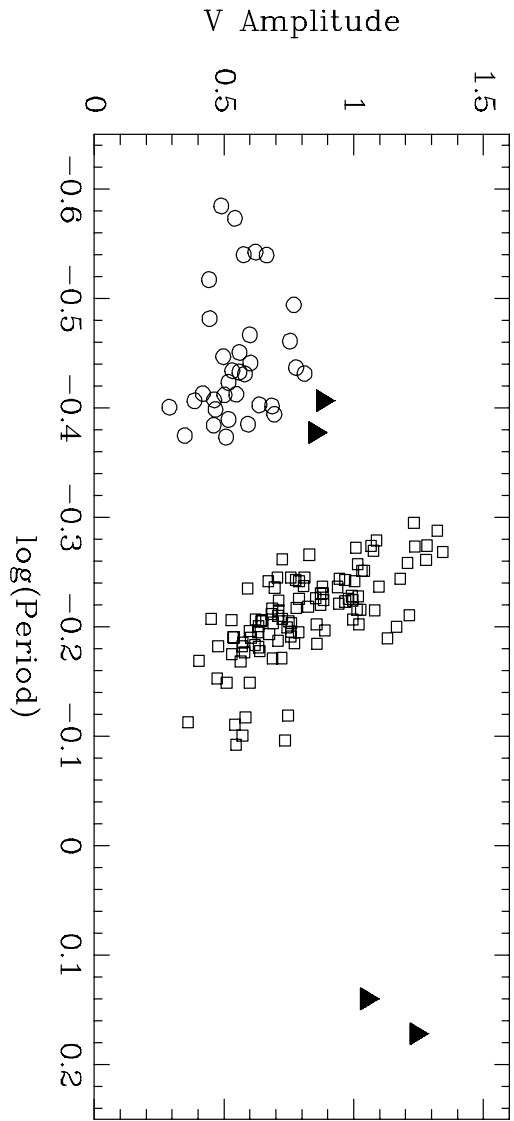
Var ID	Star ID	RA J2000.0	DEC J2000.0	Period (Days)	A_V	m_V	Bailey Type	$\Delta \log P$
V152	3834	11:13:10.49	22:07:59.2	0.39628	0.685	22.22	c	
V153	3855	11:13:13.11	22:06:31.2	0.53161	1.282	22.36	ab	-0.038
V154	3858	11:13:27.63	22:07:37.0	0.57966	1.097	22.16	ab	-0.046
V155	3899	11:13:37.02	22:10:09.5	0.57998	0.938	22.29	ab	-0.022
V156	3922	11:13:21.68	22:12:57.0	0.66558	0.580	22.19	ab	-0.026
V157	3943	11:13:32.38	22:07:20.5	0.70267	0.473	22.19	ab	-0.033
V158	3949	11:13:37.75	22:09:35.5	0.38603	0.418	22.20	c	
V159	3970	11:13:28.80	22:12:35.5	0.62165	0.648	22.18	ab	-0.007
V160	3989	11:13:18.88	22:05:50.7	0.65722	0.477	22.16	ab	-0.004
V161	4055	11:13:18.78	22:08:12.5	0.42312	0.508	22.16	c	
V162	4127	11:13:45.68	22:04:22.8	0.60893	0.711	22.33	ab	-0.007
V163	4147	11:13:11.63	22:10:37.2	0.62955	0.633	22.31	ab	-0.010
V164	4159	11:13:43.33	22:11:57.2	0.65348	0.859	22.19	ab	-0.061
V165	4165	11:13:22.33	22:06:18.2	0.61594	0.709	22.17	ab	-0.012
V166	4200	11:13:24.30	22:11:12.7	0.57983	0.879	22.33	ab	-0.012
V167	4238	11:13:08.79	22:11:16.3	0.59477	0.789	22.32	ab	-0.009
V168	4304	11:13:21.62	22:07:32.4	0.50692	1.232	22.43	ab	-0.009
V169	4331	11:13:11.79	22:11:15.5	0.26704	0.542	22.34	c	

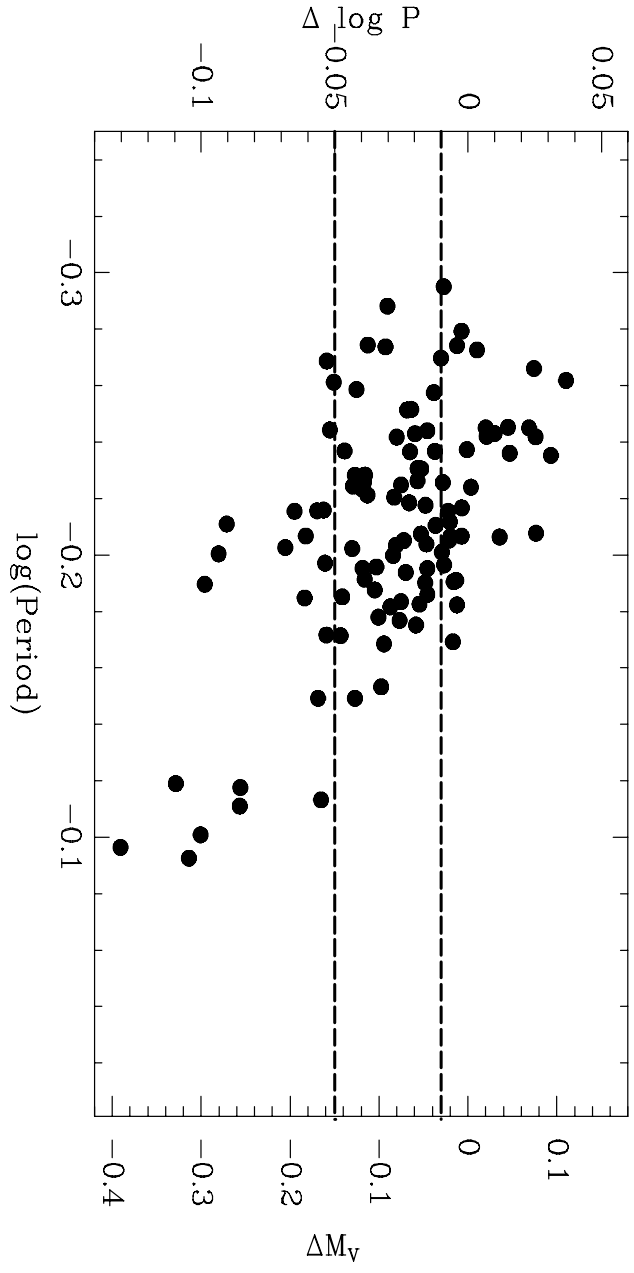
TABLE II. DI93 Stars that are non-variable

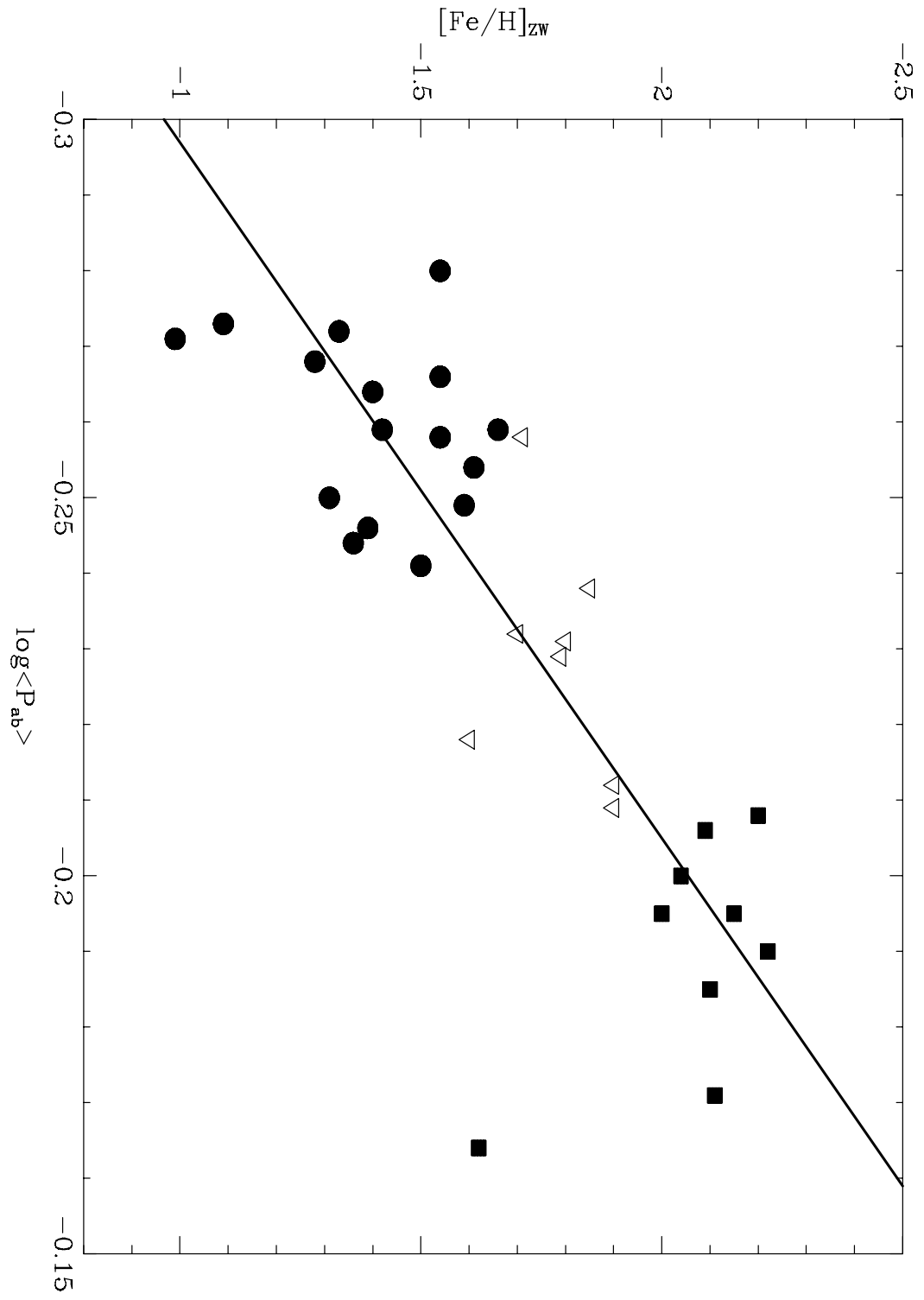
DI93 ID	Star ID	WS Index
V3	4724	1.5
V4	3541	2.3
V7	5486	1.1
V12	1103	1.5
V13	4698	1.4
V20	2365	2.8
V26	3831	1.6
V27	5673	2.9
V35	4612	1.2
V42	4057	1.3
V45	3065	0.8
V47	4421	0.9
V51	5433	1.2
V58	4224	1.2
V59	3939	1.2
V63	3890	2.0
V66	1291	1.1
V68	3558	2.7
V71	4318	2.4
V72	3445	2.7

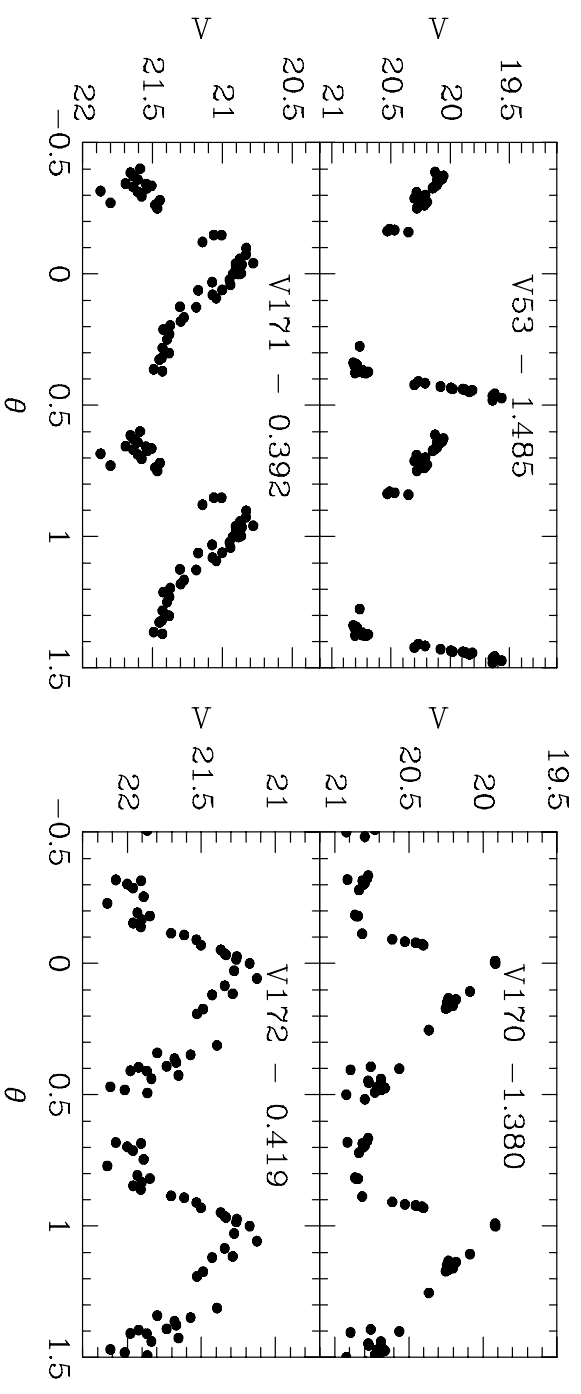
TABLE III. Anomalous Cepheids

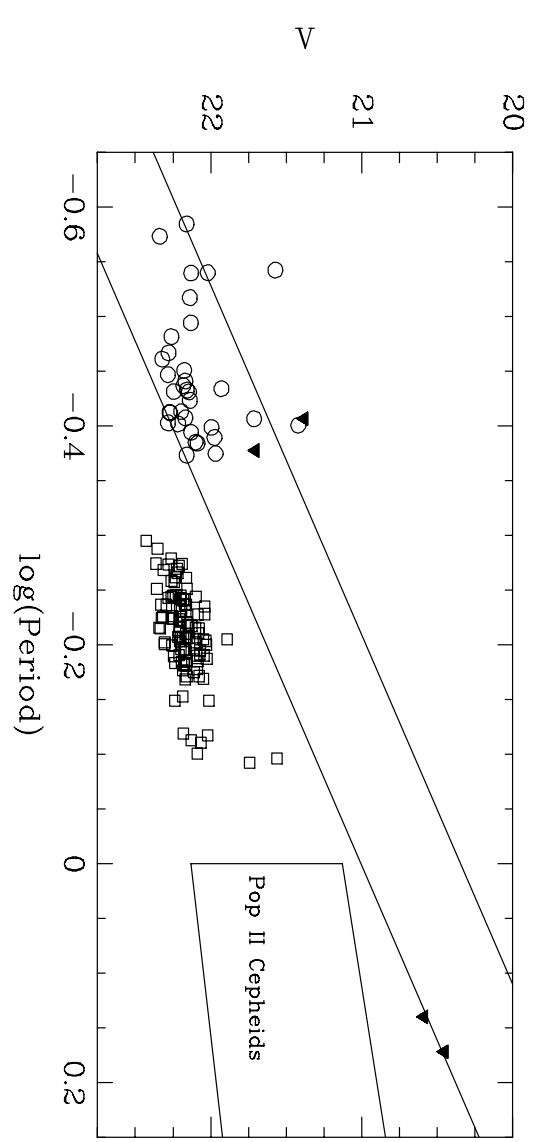
Var ID	Star ID	RA J2000.0	DEC J2000.0	Period (Days)	A_V	m_V	Pulsation Mode	Swope ID
V53	645	11:13:22.39	22:08:34.6	1.48466	1.240	20.45	Fundamental	V27
V170	737	11:13:09.58	22:10:26.3	1.37955	1.050	20.59	Fundamental	V203
V171	1205	11:13:14.54	22:11:41.6	0.39191	0.879	21.38	Overtone	V51
V172	1545	11:13:34.75	22:13:44.8	0.41907	0.850	21.70	Overtone	V1











This figure "Siegel.RRfig1.gif" is available in "gif" format from:

<http://arxiv.org/ps/astro-ph/0004099v1>

This figure "Siegel.RRpage1.gif" is available in "gif" format from:

<http://arxiv.org/ps/astro-ph/0004099v1>

This figure "Siegel.RRfig2.gif" is available in "gif" format from:

<http://arxiv.org/ps/astro-ph/0004099v1>

This figure "Siegel.RRpage2.gif" is available in "gif" format from:

<http://arxiv.org/ps/astro-ph/0004099v1>

This figure "Siegel.RRpage3.gif" is available in "gif" format from:

<http://arxiv.org/ps/astro-ph/0004099v1>

This figure "Siegel.RRpage4.gif" is available in "gif" format from:

<http://arxiv.org/ps/astro-ph/0004099v1>

This figure "Siegel.RRpage5.gif" is available in "gif" format from:

<http://arxiv.org/ps/astro-ph/0004099v1>

This figure "Siegel.RRpage6.gif" is available in "gif" format from:

<http://arxiv.org/ps/astro-ph/0004099v1>